Talanta 100 (2012) 1–6

Contents lists available at SciVerse ScienceDirect

Talanta

journal homepage: www.elsevier.com/locate/talanta

A fast and sensitive immunoassay of avian influenza virus based on label-free quantum dot probe and lateral flow test strip

Xuepu Li [a,1], Donglian Lu [a,1], Zonghai Sheng [a], Kun Chen [a], Xuebo Guo [b], Meilin Jin [b], Heyou Han [a,*]

[a] State Key Laboratory of Agricultural Microbiology, College of Science, Huazhong Agricultural University, Wuhan 430070, PR China
[b] Unit of Animal Infectious Diseases, State Key Laboratory of Agricultural Microbiology, Huazhong Agricultural University, Wuhan 430070, PR China

ARTICLE INFO

Article history:
Received 1 June 2012
Received in revised form
16 August 2012
Accepted 27 August 2012
Available online 3 September 2012

Keywords:
Quantum dots
Fluorescence immunoassay
Signal amplification
Avian influenza virus
Lateral flow test strip

ABSTRACT

A novel fluorescence immunoassay method for fast and ultrasensitive detection of avian influenza virus (AIV) was developed. The immunoassay method which integrated lateral flow test strip technique with fluorescence immunoassay used the label-free and high luminescent quantum dots (QDs) as signal output. By the sandwich immunoreaction performed on lateral flow test strip, the gold nanoparticle (NP) labels were captured in the test zone and further dissolved to release a large number of gold ions as a signal transduction bridge that was detected by the QDs-based fluorescence quenching method. Under the optimal conditions, the relative fluorescence intensity of QDs was linear over the range of 0.27–12 ng mL^{-1} AIV, and the limit of detection was estimated to be 0.09 ng mL^{-1} which was 100-fold greater than enzyme-linked immunosorbent assay (ELISA). The sensitive and specific response was also coupled with high reproducibility in the proposed method. A series of six parallel measurements produced reproducible fluorescent signals with a relative standard deviation of 4.7%. The proposed method can be used to directly detect clinical sample without any pretreatment, and showed high efficiency (90.0%), sensitivity (100.0%) and specificity (88.2%) compared with virus isolation (gold method). The new method shows great promise for rapid, sensitive, and quantitative detection of AIV in-field or point-of-care diagnosis.

1. Introduction

Avian influenza is a highly contagious disease caused by type A influenza virus. It infects not only poultry, but also causes disease in human beings, resulting in human to human transmission and triggering a global pandemic [1]. Since the first report of highly pathogenic avian influenza in Hong Kong in 1997, the number of avian influenza cases increased during the last decade [2]. According to April 2010 World Health Organization statistics, 495 people had been infected with avian influenza virus (AIV), including 292 deaths. Furthermore, it has killed millions of poultry not only in Asia but also throughout Europe and Africa [3]. Therefore, early detection of avian influenza infection in poultry is critical for aiding the control of outbreaks [4].

Recently, several methods have been developed to detect AIV including virus isolation (VI), enzyme-linked immunosorbent assay (ELISA), standard reverse transcription-polymerase chain reaction (RT-PCR), real-time RT-PCR and so on [5–8]. Among them, ELISA is one of the most popular methods for the detection of avian influenza. In ELISA, the test relies on the reaction between enzyme and substrate, and then converts it into a detectable signal. However, the colorimetry has a relative low sensitivity, thus the detection limit is very limited [9]. What's more, the assay time is relatively long and the procedure is complex due to multiple-step processes involved in the ELISA [10]. RT-PCR is a sensitive technique, but also has some disadvantages such as a complicated procedure, long assay time, high cost and high false positive rate arising from cross contaminations between samples [11,12]. The typical virus isolation method requires 5–7 days for testing, which is also a very labor-intensive and time consuming procedure.

For the sensitive, rapid and cost-effective detection of the AIV, many technologies have been developed. Combining the novel nanomaterial and the specific reaction of the antibody and antigen, many novel immunosensors have been invented as alternative tools to replace the traditional methods. Different nanomaterials have been used in the resonance light scattering [13], electrochemistry [14] and surface plasmon resonance [15,16] technology to gain the sensitive immunoassay for AIV. Though most of the reported immunosensor have shortened the analysis time, simplified the procedure with good sensitivity, nearly all of them need expensive instruments and extensive labor. These disadvantages limited their applications primarily in laboratory and prohibit their use in the field or point-of-care testing.

* Corresponding author. Tel./fax: +86 27 87288246.
E-mail address: hyhan@mail.hzau.edu.cn (H. Han).
[1] These authors contributed equally to this work.

0039-9140/$ - see front matter Crown Copyright © 2012 Published by Elsevier B.V. All rights reserved.
http://dx.doi.org/10.1016/j.talanta.2012.08.041

Lateral flow test strip (LFTS) which integrates chromatography technique with conventional immunoassay opens up a new avenue for clinical analysis [17]. This method has a number of advantages, such as (1) user-friendly format, (2) rapid detection, (3) less interference due to chromatographic separation, (4) good reproducibility, and (5) relatively low cost [18–21]. However, owing to the limits of visible judgment, LFTS is still not sensitive to detect some disease biomarkers. Therefore, it is imperative to develop a sensitive and quantitative LFTS for detecting disease biomarker accurately at an early stage of virus infection. Signal transformation and amplification are effective methods for the improvement of the sensitivity of LFTS. Several nanoparticles (NPs) such as gold NPs, silica NPs, quantum dots (QDs), and metal phosphate NPs were used as signal transduction bridges [22–27]. For example, Lin's group developed electrochemical immunosensor diagnosis device based on QD probe and IST, the biosensor employed QD label as a signal-amplifier vehicle [28]. Previously, we reported an indirect fluorescence immunoassay for the high-throughput screening of the antibody of APP [29]. The method used label-free QDs as a probe and gold ions released from gold NPs as a signal transduction bridge. In this study, we integrated the lateral flow test strip technique with the indirect fluorescence immunoassay to provide a novel method for the detection of AIV. The successful integration led the proposed method to have the advantages of both the LFTS and QDs-based fluorescence quenching method. These advantages such as sensitivity, rapid and cost-effective allowed the method to show great promise for quantitative detection of AIV in-field or point-of-care diagnosis.

2. Experimental

2.1. Reagents and apparatus

$HAuCl_4 \cdot 4H_2O$ was obtained from Shanghai Chemical Reagent Co. Ltd. (Shanghai, China). $CdCl_2 \cdot 2.5H_2O$ (99.0%) and $NaBH_4$ (96.0%) were obtained from Tianjin Chemical Reagent Plant (Tianjin, China). Na_2TeO_3 was obtained from Sinopharm Chemical Reagent Co., Ltd. (Shanghai, China). Glutathione (GSH) was purchased from Sanland-Chem. International Inc. (Xiamen, China). Polyester backing materials, glass fibers, and absorbent materials were purchased from Millipore Corp (Bedford, MA). The nitrocellulose membrane (AE 98) was obtained from Schleicher Schuell BioScience, Inc. (Keen, NH). All the AIV strains used in this study were taken from the Unit of Animal Infectious Diseases of Huazhong Agricultural University. The AIV virus subtype H5 antigen and AIV monoclonal antibody were made by our cooperator (The detailed procedure for the preparation of AIV virus and monoclonal antibody is described in the supporting information). All other reagents were of analytical reagent grade and used without further purification. Ultrapure water (18.25 MΩ cm) was used throughout the experiments.

The ultraviolet–visible (UV–vis) absorption spectra were performed on a Thermo Nicolet Corporation Model Evolution 300 spectrophotometer coupled with a 1.0 cm quartz cell. The photoluminescence (PL) spectra were obtained with a PerkinElmer Model LS-55 luminescence spectrometer equipped with a 20 kW xenon discharge lamp as a light source. The transmission electron microscopy (TEM) and high-resolution transmission electron microscopy (HRTEM) images were acquired on a JEM2010FEF HRTEM (Japan). The concentration of virus was determined by a DU 800 UV–vis spectrophotometer (Beckman Coulter, USA). The PL intensity was detected by a Biotech Corporation Model Synergy HT multi-detection microplate reader (Excitation at 390 nm, Emission at 540 nm).

2.2. Synthesis of GSH-capped CdTe QDs

The GSH-capped CdTe QDs were prepared according to our previously reported method [30]. In a typical synthesis, cadmium chloride ($CdCl_2 \cdot 2.5H_2O$, 0.5 mmol) was dissolved in 50 mL ultrapure water in a two-necked flask, and GSH (0.6 mmol), trisodium citrate dihydrate (0.17 mmol), Na_2TeO_3 (0.1 mmol) and $NaBH_4$ (0.48 mmol) were added under vigorous stirring, and then the pH was adjusted to 10.5 by adding saturated NaOH solution. When the color of the solution changed to light green, the mixture was refluxed for 1 h at 100 °C and the growth of CdTe QDs took place immediately. The Nicolet Evolution 300 Ultraviolet–Visible spectrometer and PerkinElmer Model LS-55 luminescence spectrometer were used to measure the UV–vis absorption spectrum, PL spectrum of the QDs respectively. The TEM image of the QDs was also characterized. All the results are shown in Figs. S1 and S2 (in supporting information).

2.3. Synthesis of gold NPs

Gold NPs were synthesized by the citrate reduction method. All glassware used were thoroughly cleaned with HNO_3–HCl solution (3 parts HCl, 1 part HNO_3), rinsed with ultrapure water and dried in oven. Briefly, 0.01% solution (100 mL) of $HAuCl_4 \cdot 4H_2O$ was brought to boiling and 3 mL of 1% (wt) solution of sodium citrate was added to the boiling solution under vigorous stirring. When the color changed from light yellow to brilliant red, the solution was boiled for another 5 min to complete the reduction of the $HAuCl_4$. After cooling to room temperature, the gold colloid solution was diluted to 100 mL using deionized water.

2.4. Preparation of gold NPs–antibody conjugate

Gold NPs–antibody conjugate was prepared according to our previously reported method [31,32]. Gold NPs (0.5 mL) were mixed with the AIV monoclonal antibody (0.5 mL) for 2 h. The mixture solution was purified by centrifugation at 15,000*g* for 1 h, and the soft sediment was resuspended in sodium phosphate buffered saline (0.1 mol L^{-1}, pH 7.2–7.4) and stored at 4 °C.

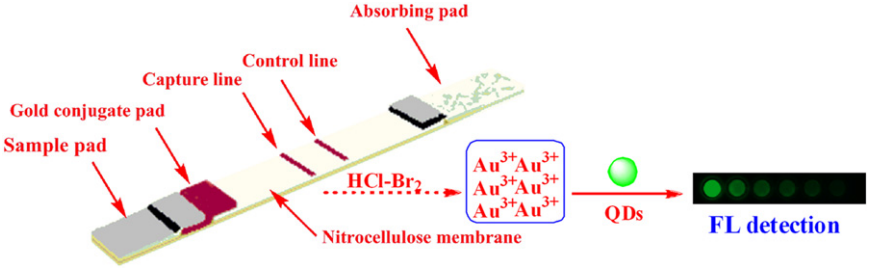

Scheme 1. The principle of the indirect fluorescence immunoassay method for detection of AIV.

2.5. Preparation of the colloidal gold LFTS

The colloidal gold LFTS was prepared using our previously reported method [33]. A typical procedure was as follows: the gold NPs–antibody conjugate solution was dispensed onto glass fiber paper using an XYZ3050 Dispense Workstation (BioDot, Inc., Sky Park, Irvine, CA.), and the conjugate pad was dried under vacuum. The solutions of AIV monoclonal antibody and rabbit anti-chicken secondary antibody were dispensed onto nitrocellulose membrane strip at the test and control zones respectively. After drying for 2 h at 37 °C, the membrane strips were blocked by incubating in 0.02 mol L^{-1} sodium phosphate buffered saline (pH 7.5) containing 2% (w/v) nonfat dried milk for 25 min and washed 3 times with PBS containing 0.1% (v/v) Tween-20. The membrane was dried for 2 h at 37 °C and stored at 4 °C. Finally, the sample pad, conjugate pad, nitrocellulose membrane, and absorbent pad were glued together on a backing plate (300 × 70 mm), and then cut into 3-mm-wide strips using a CM-4000 cutter (BioDot, Inc., Sky Park, Irvine, CA.) (Fig. S3 in supporting information). The strip was stored at 4 °C until required.

2.6. Procedures for the determination of AIV

100 μL sample solution containing a desired concentration of AIV was applied to the sample pad. After waiting for 10 min, two red bands were drawn at the test and control zones. After that, 200 μL HCl–Br_2 solution was dropped into the test zone to release gold ions from the captured gold NP labels. Then the obtained solution containing gold ions was collected with a 96-well microplate. After volatilization of the residual HCl–Br_2 solution, 100 μL QD solution was added to 96-well microplate and the fluorescent signals were recorded by the Biotech Corporation Model Synergy HT multi-detection microplate reader. Considering any potential danger caused by the AIV, all the rejected and recycled materials were need to be heat inactivated after measurement.

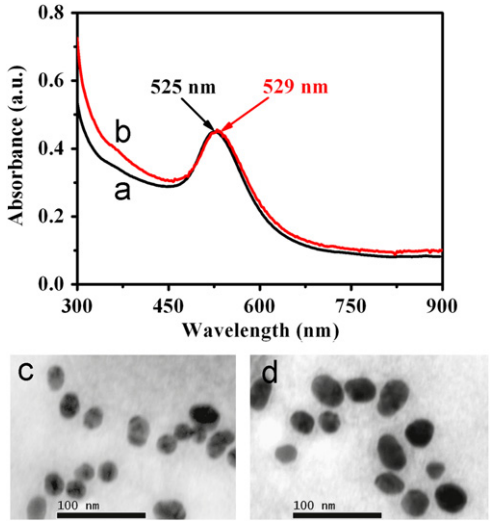

Fig. 1. UV–vis absorption spectra of gold NPs (a), gold NPs–antibody conjugate (b), TEM images of gold NPs (c) and gold NPs–antibody conjugate (d).

3. Results and discussion

3.1. Principle of the indirect fluorescence immunoassay

Scheme 1 illustrates the principle of the indirect fluorescence immunoassay for measuring the AIV. The immunoassay system mainly consists of two parts: colloidal gold LFTS and fluorescent detection system. The LFTS consists of sample pad, gold NP–antibody conjugate pad, nitrocellulose membrane and absorbent pad. During the assay, the sample solution (100 μL) containing AIV was first added onto the sample pad. Subsequently, the liquid sample migrated toward gold NPs–antibody conjugate pad by capillary action. Then the binding between the gold NPs–antibody conjugate and AIV occurred, and the formed complexes continued to migrate along the strip. Once reaching the test zone, the complexes were captured by the antibody immobilized on the test zone via interaction between antibody and antigen. Then the excess gold NPs–antibody conjugate migrated further and was captured on the control zone via antibody-second antibody immunoreaction. Finally, the gold NPs at the test zone were dissolved in 200 μL HCl–Br_2 mixed solution to release gold ions, which were collected with a 96-well microplate. QDs were added to 96-well microplate after volatilizing the residual HCl–Br_2 and the fluorescent signals were recorded by the Biotech Corporation Model Synergy HT multi-detection microplate reader. The concentration of AIV is proportional to the relative fluorescence intensity of QDs.

3.2. Characterization of gold NPs–antibody conjugate

The preparation and biological activity of the gold NPs–antibody conjugate usually affected the results of the immunoassay for AIV. In the current study, the antibody of AIV was linked to the surface of gold NPs through electrostatic interaction to form gold NPs–antibody conjugate. Compared with the QDs–antibody conjugate, the preparation process is simple, efficient, and does not use any coupling agent. The obtained conjugates were characterized by UV–vis absorption spectra and TEM image. Line a in Fig. 1 showed a typical UV–vis absorption spectrum of gold NPs. A sharp surface plasmon absorption band is located at

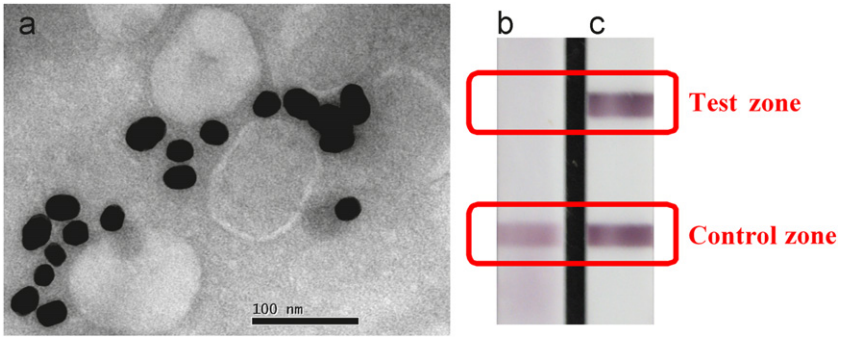

Fig. 2. TEM image of gold NPs–antibody conjugate in the presence of AIV using negative-staining method (a), and qualitative analysis result of the colloidal gold LFTS (b: blank, c: sample solution contained AIV).

525 nm. Due to the strong electrostatic interaction between gold NPs and antibody, the surface plasmon absorption band of gold NPs shifted from 525 to 529 nm, which indicated that the gold NPs–antibody conjugate was formed (Fig. 1 Line b). The TEM further verified the conjugation; the as-prepared gold NPs are uniform in size with an average particle size of 22 nm (Fig. 1c) while after conjugation with antibody, the average particle size of gold NPs increased to 30 nm (Fig. 1d). The homogeneous distribution also demonstrated the good stability of the conjugate.

3.3. Biological activity of gold NPs–antibody conjugate

The biological activity of gold NPs–antibody conjugate was studied using TEM image. The mixed solution of the conjugate and AIV was dropped on the surface of a carbonate support film of the TEM grid, and was negatively stained using phosphotungstic acid (1.0%). The results showed that the as-prepared conjugate was successfully attached to the surface of AIV which has an average particle size of 100 nm and a similar spherical morphology (Fig. 2a). Moreover, qualitative analysis results of the as-prepared colloidal gold LFTS also exhibited that the as-prepared gold NPs–antibody conjugate pad has a highly biological activity. As shown in Fig. 2c, when the sample solution containing AIV was added to the sample pad, after several minutes, two red bands could be observed on the test and control zones. On the contrary, no characteristic red band was observed on the test zone for the non-infected serum (without AIV) (Fig. 2b). Therefore, the above results showed that the prepared colloidal gold LFTS had high quality and could also be used to qualitatively detect AIV.

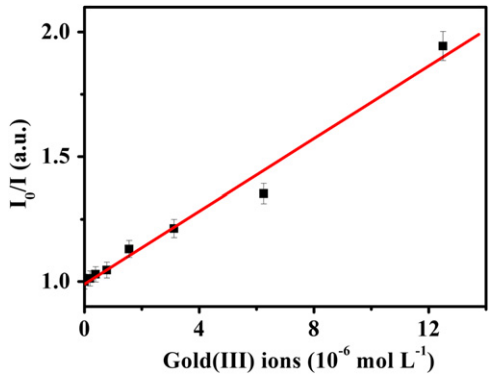

Fig. 3. Effect of gold ion concentration on the I_0/I of CdTe QDs. (I_0 and I are the fluorescent intensity of QDs in the absence and presence of gold ions, respectively). Each point depicted the average measurements of three times. Error bars were calculated based on the standard deviation of three measurements.

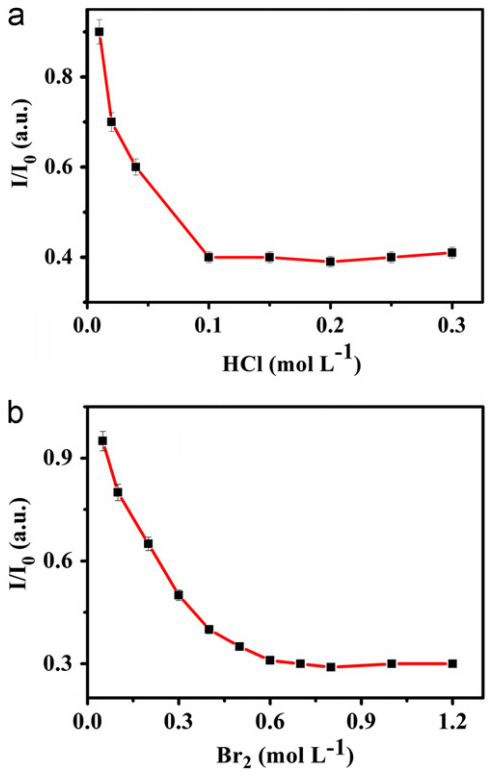

Fig. 4. Effects of the concentrations of HCl (a) and Br_2 (b) on the relative fluorescence intensity of CdTe QDs (I/I_0). Each point depicted the average measurements of three times. Error bars were calculated based on the standard deviation of three measurements.

3.4. Fluorescence quenching effect of gold ions on CdTe QDs

In the following experiments, the fluorescent quenching ability of gold ions dissolved from the gold NPs–antibody conjugate was investigated using a 96-well microplate reader. The results showed that the released gold ions quenched the fluorescence of QDs in a concentration dependence which is best described by a Stern–Volmer type equation: $I_0/I = 1 + K_{sv}$ [gold ions]. I_0 and I are the fluorescent intensity of QDs in the absence and presence of gold ions, respectively. K_{sv} is a Stern–Volmer quenching constant. As shown in Fig. 3, the ratio of fluorescent intensity of QDs (I_0/I) was linear with the concentration of gold ions over the range of 0.2–6.25 μmol L^{-1} and the detection limit was 68 nmol L^{-1}. K_{sv} value was 7.3×10^4 L mol^{-1}. The results indicated that the released gold ion has highly fluorescent quenching ability. Therefore, as a signal transduction and amplification bridge, it would

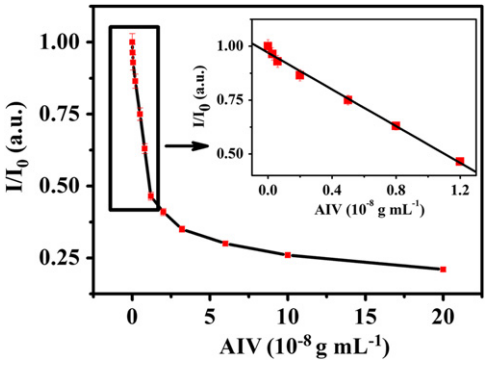

Fig. 5. The concentration of AIV versus the relative fluorescence intensity (I/I_0) of QDs. Inset shows the linear relationship of the concentration of AIV and the relative fluorescence intensity of QDs. Each point depicted the average measurements of three times. Error bars were calculated based on the standard deviation of three measurements.

Table 1
Comparison of different methods for the determination of AIV antigen.

Technique	Linear range (ng mL^{-1})	Detection limit (ng mL^{-1})	Reference
Fluoroimmunoassay	8–510	0.15	[10]
ELISA	–	5	[10]
ELISA	–	10	[34]
Electrochemistry	–	5×10^3	[35]
DAS-ELISA	–	2.5	[36]
RLS	0.5–50	0.15	[13]
Indirect fluorescence immunoassay	0.27–12	0.09	This work

Table 2
Comparative results of the proposed method and virus isolation of 20 clinical samples.

		Virus isolation			Performance				
		Positive	Negative	Total	Efficiency[a] (%)	Sensitivity[b] (%)	Specificity[c] (%)	FP rate[d] (%)	FN rate[e] (%)
The proposed method	Positive	3.0	2.0	5.0	90.0	100.0	88.2	11.8	0.0
	Negative	0.0	15.0	15.0					
	Total	3.0	17.0	20.0					

[a] Efficiency = (TP + TN) × 100/Total.
[b] Sensitivity = TP × 100/(TP + FN).
[c] Specificity = TN × 100/(TN + FP).
[d] False-positive rate = FP × 100/(FP + TN).
[e] False-negative rate = FN × 100/(TP + FN).

play an important role in connecting the fluorescent signal of QDs and the concentration of AIV, and improving the sensitivity of the indirect fluorescence immunoassay.

3.5. Optimization of experimental conditions

To achieve high sensitivity and minimize the interferential signal for the detection of AIV, we investigated the effect of the concentrations of HCl and Br_2 on the dissolution of gold NPs at the test zone. The concentration of gold nanoparticles used in the experimental was 8 nmol L^{-1}. As shown in Fig. 4a, with increasing the concentration of HCl, the relative fluorescence intensity of QDs decreased and reached a plateau in the concentration of 0.1–0.3 mol L^{-1}. A similar result was obtained for Br_2 (Fig. 4b). So 0.15 mol L^{-1} HCl and 0.8 mol L^{-1} Br_2 were used for further experiments.

3.6. Analytical performance of the fluorescence immunoassay

Under the optimized condition, the proposed method was used to quantitatively detect AIV. As shown in Fig. 5, the relative fluorescence intensity decreased with increasing concentration of AIV. After the concentration of AIV reached 60 ng mL^{-1}, the relative fluorescence intensity still had a slight decrease but tend to be stable. The main reason may be the hook effect caused by high AIV level which is an intrinsic problem of single step sandwich-type immunoassay. The linear range for the concentration of AIV was found to be 0.27–12 ng mL^{-1} (Inset Fig.) and the detection limit was 0.09 ng mL^{-1} (S/N = 3). The sensitivity of the proposed method was not only superior to the traditional method of ELISA but also comparable with some reported novel immunosensor (see Table 1).

The precision of the proposed method was further evaluated by a series of six parallel measurements with the same batch of LFTS at a concentration of 80 ng mL^{-1}. The immunoassay produced reproducible fluorescent signals with a relative standard deviation of 4.7% (data not shown), indicating acceptable fabrication reproducibility. The assay time (30 min) with the novel fluorescence immunoassay was also less than most of the reported methods, such as virus isolation (gold method), conventional ELISA and fluorescence immunoassay [10]. The successful integration led the proposed method to have the advantages of both the LFTS and QDs-based fluorescence quenching method. Compared with the ELISA and virus isolation, the proposed method shortened the analysis time, simplified the procedure with good sensitivity. What's more, the procedure is very simple and easy to learn, the cost of per lateral flow test strip was approximately 0.3 dollar which was cheaper than most of the reported method. To obtain an accurate quantitative result, it was not limited in the well-equipment laboratory; a common luminescence spectrometer was adequate.

3.7. Analysis of AIV in real serum samples

The virus isolation which is regarded as the gold standard method is the most commonly used method in the AIV detection. To evaluate the diagnostic performance of the proposed indirect fluorescence immunoassay, we compared the results of the proposed method with the virus isolation. 20 clinical samples which were collected from naturally infected chicken and without any appropriate reference tests to classify them into truly infected and non-infected were analyzed by the proposed method and virus isolation. As shown in Table 2, compared with virus isolation the proposed method had an efficiency of 90.0%, sensitivity of 100.0% and specificity of 88.2%. Moreover, the false positive and negative rates were 11.8% and 0.0%, respectively. The results showed that the proposed indirect fluorescence immunoassay method with high sensitivity and specificity can be used to detect AIV in clinical diagnostic test.

4. Conclusions

In conclusion, an indirect fluorescence immunoassay method for simple, rapid and sensitive detection of AIV was developed based on the label-free QD probe and lateral flow test strip strip. The method combined the benefits of LFTS and high sensitivity of QDs-based fluorescence quenching method, and has been successfully applied for the detection of AIV with a detection limit of 0.09 ng mL^{-1}. Compared with the virus isolation method (gold method), the results of clinical sample analysis showed high consistency. The novel indirect fluorescence immunoassay provided a new approach for highly sensitive and specific detection of AIV, and showed potential applications in early diagnosis of animal epidemic diseases in clinic. Further work will allow a more cheap, simple and convenient portable device for commercial applications.

Acknowledgment

The authors gratefully acknowledge the financial support for this research from National Natural Science Foundation of China (20975042, 21175051), the Fundamental Research Funds for the Central Universities (2010PY009, 2010PY139) and the Natural Science Foundation of Hubei Province Innovation Team (2011CDA115).

Appendix A. Supporting information

Supplementary data associated with this article can be found in the online version at http://dx.doi.org/10.1016/j.talanta.2012.08.041.

References

[1] Z.J. Yu, Y.F. Song, H.B. Zhou, X.J. Xu, Q.Y. Hu, H.Y. Wu, A.D. Zhang, Y.J. Zhou, J.F. Chen, H.B. Dan, Q.P. Luo, X.X. Li, H.C. Chen, M.L. Jin, Emerg. Infect. Dis. 13 (2007) 772–775.
[2] Y. Guan, J.S.M. Peiris, A.S. Lipatov, T.M. Ellis, K.C. Dyrting, S. Krauss, L.J. Zhang, R.G. Webster, K.F. Shortridge, Proc. Natl. Acad. Sci. USA 99 (2002) 8950–8955.
[3] S. Cui, C. Chen, G. Tong, J. Virol. Methods 152 (2008) 102–105.
[4] C. Cao, R. Dhump, D.D. Bang, Z. Ghavifekr, J. Høgberg, A. Wolff, Analyst 135 (2010) 337–342.
[5] J.F. Chen, M.L. Jin, Z.J. Yu, H.B. Dan, A.D. Zhang, Y.F. Song, H.C. Chen, J. Vet. Diagn. Invest. 19 (2007) 155–160.
[6] Q. He, S. Velumani, Q. Du, C.W. Lim, F.K. Ng, R. Donis, J. Kwang, Clin. Vaccine Immunol. 14 (2007) 617–623.
[7] Q.P. Luo, H.L. Huang, W. Zou, H.B. Dan, X.G. Guo, A.D. Zhang, Z.J. Yu, H.C. Chen, M.L. Jin, Vet. Microbiol. 137 (2009) 24–30.
[8] S. Velumani, Q. Du, B.J. Fenner, M. Prabakaran, L.C. Wee, L.Y. Nuo, J. Kwang, J. Virol. Methods 147 (2008) 219–225.
[9] M. Nichkova, J. Feng, F. Sanchez-Baeza, M.P. Marco, B.D. Hammock, I.M. Kennedy, Anal. Chem. 75 (2003) 83–90.
[10] L.P. Chen, Z.H. Sheng, A.D. Zhang, X.B. Guo, J.K. Li, H.Y. Han, M.L. Jin, Luminescence 25 (2010) 419–423.
[11] J. Pasick, Transboundary Emerg. Dis. 55 (2008) 329–338.
[12] M. Munch, L.P. Nielsen, K. Handberg, P.H. Jørgensen, Arch. Virol. 146 (2001) 87–97.
[13] X. Zou, H. Huang, Y. Gao, X.G. Su, Analyst 137 (2012) 648–653.
[14] Y.X. Li, M. Hong, Y.Q. Lin, Q. Bin, Z.Y. Lin, Z.W. Cai, G.N. Chen, Chem. Commun. 48 (2012) 6562–6564.
[15] D.J. Schofield, N.J. Dimmock, J. Virol. Methods 62 (1996) 33–42.
[16] P. Critchley, N.J. Dimmock, Bioorg. Med. Chem. 12 (2004) 2773–2780.
[17] P. Yager, T. Edwards, E. Fu, K. Nelson, M. Tam, B.H. Weigl, Nature 442 (2006) 412–418.
[18] Y. Guo, B. Ngom, T. Le, X. Jin, L. Wang, D. Shi, X. Wang, D. Bi, Anal. Chem. 82 (2010) 7550–7555.
[19] B.H. Liu, Z. Tsao, J.J. Wang, F.Y. Yu, Anal. Chem. 80 (2008) 7029–7035.
[20] X. Mao, Y. Ma, A. Zhang, L. Zhang, L. Zeng, G. Liu, Anal. Chem. 81 (2009) 1660–1668.
[21] H. Xu, X. Mao, Q. Zeng, S. Wang, A.N. Kawde, G. Liu, Anal. Chem. 81 (2009) 669–675.
[22] R. Cui, H.C. Pan, J.J. Zhu, H.Y. Chen, Anal. Chem. 79 (2007) 8494–8501.
[23] A.P. Fan, C. Lau, J.Z. Lu, Anal. Chem. 77 (2005) 3238–3242.
[24] G. Liu, H. Wu, J. Wang, Y. Lin, Small 2 (2006) 1139–1144.
[25] G. Liu, Y. Lin, J. Am. Chem. Soc. 129 (2007) 10394–10401.
[26] H.F. Chen, D.P. Tang, B. Zhang, B.Q. Liu, Y.L. Cui, G.N. Chen, Talanta 91 (2012) 95–102.
[27] K. Pinwattana, J. Wang, C.T. Lin, H. Wu, D. Du, Y. Lin, O. Chailapakul, Biosensors Bioelectron. 26 (2010) 1109–1113.
[28] G. Liu, Y. Lin, J. Wang, H. Wu, C.M. Wai, Y. Lin, Anal. Chem. 79 (2007) 7644–7653.
[29] Z.H. Sheng, H.Y. Han, D.H. Hu, J.G. Liang, Q.G. He, M.L. Jin, R. Zhou, H.C. Chen, Chem. Commun. 18 (2009) 2559–2561.
[30] Z.H. Sheng, H.Y. Han, X.F. Hu, C. Chi, Dalton Trans. 39 (2010) 7017–7020.
[31] D.H. Hu, H.Y. Han, R. Zhou, F. Dong, W.C. Bei, F. Jia, H.C. Chen, Analyst 133 (2008) 768–773.
[32] H.M. Zhang, W.T. Li, Z.H. Sheng, H.Y. Han, Q.G. He, Analyst 135 (2010) 1680–1685.
[33] J.X. Yang, M.L. Jin, J.F. Chen, Y. Yang, P. Zheng, A.D. Zhang, Y.F. Song, H.B. Zhou, H.C. Chen, J. Vet. Diagn. Invest. 19 (2007) 355–361.
[34] B. Mu, X. Huang, P. Bu, J. Zhuang, Z. Cheng, J. Feng, D. Yang, C. Dong, J. Zhang, X. Yan, J. Virol. Methods 169 (2010) 282–289.
[35] M.F. Diouani, S. Helali, I. Hafaid, W.M. Hassen, M.A. Snoussi, A. Ghram, N. Jaffrezic-Renault, A. Abdelghani, Mater. Sci. Eng. C 28 (2008) 580–583.
[36] A. Zhang, M.L. Jin, F.F. Liu, X.B. Guo, Q.Y. Hu, L. Han, Y.D. Tan, H.C. Chen, Avian Dis. 50 (2006) 325–330.